International Journal of Antimicrobial Agents 49 (2017) 74–80

Contents lists available at ScienceDirect

International Journal of Antimicrobial Agents

journal homepage: www.elsevier.com/locate/ijantimicag

Multi-omics approach to study global changes in a triclosan-resistant mutant strain of *Acinetobacter baumannii* ATCC 17978

Dinesh M. Fernando [a], Patrick Chong [b], Manu Singh [a], Victor Spicer [c], Mark Unger [a], Peter C. Loewen [a], Garrett Westmacott [b], Ayush Kumar [a,d,*]

[a] Department of Microbiology, University of Manitoba, Winnipeg, MB R3T 2N2, Canada
[b] National Microbiology Laboratory, Public Health Agency of Canada, Winnipeg, MB, Canada
[c] Department of Internal Medicine, University of Manitoba, Winnipeg, MB R3T 2N2, Canada
[d] Department of Medical Microbiology, University of Manitoba, Winnipeg, MB R3T 2N2, Canada

ARTICLE INFO

Article history:
Received 3 August 2016
Accepted 1 October 2016

Keywords:
Genomics
RNA-Seq
Proteomics
Global gene response

ABSTRACT

Acinetobacter baumannii AB042, a triclosan-resistant mutant strain, was examined for modulated gene expression using whole-genome sequencing, transcriptomics and proteomics in order to understand the mechanism of triclosan resistance as well as its impact on *A. baumannii*. Data revealed modulated expression of the fatty acid metabolism pathway, co-factors known to play a role in the synthesis of fatty acids, as well as several transcriptional regulators. The membrane composition of the mutant revealed a decrease in C_{18} with a corresponding increase in C_{16} fatty acids compared with the parent strain *A. baumannii* ATCC 17978. These data indicate that *A. baumannii* responds to triclosan by altering the expression of genes involved in fatty acid metabolism, antibiotic resistance and amino acid metabolism.

1. Introduction

Acinetobacter baumannii is a Gram-negative coccobacillus that has gained widespread attention due to its significant ability to resist multiple antibiotics. This opportunistic pathogen has been known to cause severe infections, due in part to its dynamic ability to generate multidrug resistance to multiple classes of antibiotics [1] and to persist in otherwise sterile environments [2]. The organism has been shown to survive stressful conditions, including desiccation [3] and growth on abiotic surfaces [4].

Triclosan [5-chloro-2-(2,4-dichlorophenoxy)phenol] is a synthetic bisphenol compound that has gained significant popularity due to its broad-spectrum efficacy, targeting type II fatty acid biosynthesis. The biocide has a specific mechanism of action occurring through inhibition of the enoyl-(acyl-carrier-protein) reductase (FabI) enzyme [5]. This enzyme is involved in fatty acid elongation by reduction of enoyl-ACP to acyl-ACP [6]. Triclosan-mediated inhibition of FabI prevents substrate binding and dissociation of the NADH co-factor forming a stable ternary structure [5], inhibiting fatty acid synthesis. Subsequent resistance to triclosan is widely reported in Gram-positive and Gram-negative bacteria, primarily caused by point mutation in *fabI*, generating an amino acid mutation (Gly→Val) [5,7,8]. Triclosan resistance also results from the activity of efflux pumps, primarily those belonging to the resistance–nodulation–division (RND) efflux pumps [9–11]. This phenomenon is associated with a multidrug-resistant phenotype [12–14].

In a previous study [15], we described a triclosan-resistant mutant (AB042) of *A. baumannii* ATCC 17978 and showed that triclosan resistance is a result of a mutation in *fabI* and overexpression of the AdeIJK RND efflux pump. In the current study, global changes in AB042 were examined using a multi-omics approach in order to understand the impact of triclosan resistance on *A. baumannii*.

2. Materials and methods

2.1. Bacterial strains and growth medium

A. baumannii AB042 has been described previously [15]. The wild-type parent strain *A. baumannii* ATCC 17978 was used as the control strain. The minimum inhibitory concentrations (MICs) of triclosan for ATCC 17978 and AB042 are 8 μg/mL and 256 μg/mL, respectively. Bacterial strains were routinely cultured in Luria–Bertani (LB) medium (Difco, BD-Canada, Mississauga, ON, Canada) at 37 °C with shaking (200 rpm unless indicated otherwise).

2.2. Fatty acid extraction and analysis

Fatty acid extraction was carried out using a previously described protocol [16] with slight modifications. Strains AB042 and ATCC 17978 were grown overnight from a single colony in 100 mL of LB medium for 16–18 h at 37 °C with shaking. The absorbance

* Corresponding author. Department of Microbiology, University of Manitoba, Winnipeg, MB R3T 2N2, Canada. Fax: +1 204 474 7603.
E-mail address: Ayush.Kumar@umanitoba.ca (A. Kumar).

http://dx.doi.org/10.1016/j.ijantimicag.2016.10.014
0924-8579/

at 600 nm (A_{600}) was equalised to 1.0 and then 50 mL of cells was harvested by centrifugation at 6000 × *g* for 15 min, was washed twice with 1 mL of phosphate-buffered saline (PBS) in pre-weighed 1.5 mL tubes, and the supernatant was removed. Pellets were re-spun and excess PBS was removed by pipette, and the pellets were placed in a dry bath at 42 °C overnight to remove moisture for dry weight measurement. Dried cell pellets in excess of 20 mg were re-suspended in 15% H_2SO_4/methanol at 10 mg/mL (Thermo Fisher Scientific, Mississauga, ON, Canada) and were transferred to a glass tube with cap. The mixture was heated at 70 °C for 3–5 h followed by addition of 1 mL of Milli-Q H_2O. Samples were left overnight to equilibrate into organic and aqueous phases. On the following day, the lower organic phase was transferred into gas chromatography vials for gas chromatography analysis, which was carried out in the Analytical Laboratory at the Department of Human Nutritional Sciences, University of Manitoba (Winnipeg, MB, Canada). Data are presented as the abundance of each fatty acid expressed as a percentage of the total of all fatty acids.

2.3. Genomic DNA extraction and sequencing

Genomic DNA was extracted from a 2 mL overnight culture using an UltraClean® Microbial DNA Isolation Kit (MO BIO Laboratories Inc., Carlsbad, CA) following the manufacturer's instructions. *A. baumannii* AB042 was sequenced using the Pacific Biosciences (PacBio) platform at the McGill University Innovation Centre for sequencing (Montreal, QC, Canada). De novo assembly of raw reads (paired ends of 151 bp each) from *A. baumannii* ATCC 17978 was carried out via the PATRIC online server using Genome Assembly tool [17]. Assembly of ATCC 17978 provided 31 contigs; AB042 was assembled into 1 contig. Contigs obtained from de novo-assembled ATCC 17978 were joined into one scaffold using the online tool CONTIGuator (http://contiguator.sourceforge.net/) [18]. For mutation analysis, the reads of AB042 were also aligned using the published *A. baumannii* ATCC 17978-mff sequence (GenBank ID **CP012004.1**) using RS_BridgeMapper pipeline available in SMRT portal. Mutations [single nucleotide polymorphisms (SNPs) and insertions and deletions (InDels)] were verified along with their positions by aligning the identified mutations against the single scaffold obtained from de novo-assembled ATCC 17978 and AB042 using the National Center for Biotechnology Information (NCBI) aligning online server. Sanger sequencing to confirm the presence of SNPs was carried out at the McGill University Innovation Centre for Sequencing. The sequence of *A. baumannii* ATCC 17978 has been deposited at DDBJ/ENA/GenBank under accession no. **LOIA00000000** (BioSample SAMN04273153).

2.4. RNA sequencing (RNA-Seq) and analysis

For transcriptomic analysis, RNA was extracted using an RNeasy RNA Extraction Kit (QIAGEN, Mississauga, ON, Canada) following the manufacturer's instructions. Briefly, a total of 1.5 mL of mid-log phase culture (A_{600} = 0.6–0.8) was spun down at 10,000 × *g* for 2 min and the supernatant was removed. The pellets were frozen overnight at –80 °C to facilitate cell lysis. RNA extraction was performed the following day and sequencing was carried out for two biological replicates of each strain at the Children's Hospital Research Institute of Manitoba (Winnipeg, MB, Canada) using an MiSeq platform (Illumina Inc., San Diego, CA). The quality of raw reads (paired ends of 151 bp each) was analysed using FastQC, and reads with a Phred score of >30 were selected for further analysis without trimming ends. Alignments were carried out using Burrows–Wheeler Alignment [19] and TopHat2 [20] command-based tools. Gene expression was quantified using the Cufflink pipeline [21]. Statistical analysis was carried out using integrated software in the Cufflink pipeline. RNA-Seq data have been submitted to the Gene Expression Omnibus (GEO) repository of NCBI under accession no. **GSE87398**.

2.5. Proteomic analysis

A total of 5 mL of overnight cultures of AB042 and ATCC 17978, inoculated from single colonies, were diluted 1:100 in 500 mL of LB broth and were incubated at 37 °C with shaking at 250 rpm to an A_{600} of ca. 0.8. Cells were pelleted at 6000 × *g* for 15 min at 4 °C and the pellets were stored at –80 °C until used. All strains were grown independently in three biological replicates. Further processing and mass spectroscopy (MS) analysis was carried out by the Mass Spectrometry and Proteomics Core at the National Microbiology Laboratory (Public Health Agency of Canada, Winnipeg, MB, Canada). Thawed cell pellets were homogenised in sterile Milli-Q H_2O, were mixed with 100 µL of 0.1 mm glass beads (Scientific Industries Inc., Bohemia, NY), were heated for 5 min at 95 °C and were vortexed vigorously for 3 min, followed by centrifugation and removal of the supernatant into a 15 mL conical tube. Cold sterile Milli-Q H_2O was added to the beads, followed by vortexing/centrifugation to wash the beads and to extract protein (total of six wash/extraction steps); the supernatant from each step was pooled together, mixed thoroughly and stored at –80 °C.

Protein was quantified using a Bicinchoninic Acid Protein Assay Kit (Pierce Protein Research Products, Thermo Fisher Scientific), with bovine serum albumin as standard. A total of 100 µg of protein from each sample was digested following a protocol described previously [22].

Each peptide sample was analysed using a nano-flow EASY-nLC™ II in-line to an LTQ (linear trap quadropole) Orbitrap Velos™ mass spectrometer (Thermo Fisher Scientific) with a nano-electrospray ion source at 2.35 kV. The peptide sample (1 µg) was loaded (30 µL at 250 bar) onto a C_{18}-reversed phase trap column (3 cm long, 100 µm inner diameter, 5.0 µm particles) with 100% nano-LC buffer A and was then separated on a C_{18}-reversed phase column (15 cm long, 75 µm inner diameter, 2.4 µm particles). Both columns were packed in-house with ReproSil-Pur C_{18}-AQ resin (Dr Maisch GmbH, Ammerbuch, Germany) and were fritted with Kasil. Peptides were eluted using a 220-min linear gradient of 2–32% nano-LC buffer B (98% acetonitrile, 0.1% formic acid) at a constant flow rate of 250 nL/min. The total nano-LC/MS/MS run time was 260 min, including the loading, linear gradient, 15-min column wash at 95% buffer B, and the column re-equilibrations.

The full MS survey scans were acquired in the Orbitrap over m/z 300–1700 with a target resolution of 60,000 at m/z 400. A data-dependent acquisition method was used, dynamically choosing the top 10 abundant precursor ions from each survey scan with an isolation width of m/z 2 for fragmentation by collision-induced dissociation (CID). The intensity threshold for selecting a precursor ion for fragmentation was 1e4 ions, with dynamic exclusion for 15 s. The fragment ion MS2 scans were acquired in the LTQ ion trap over a dynamic m/z range. Lock mass was used with polysiloxane at 371.101 m/z.

Peptide samples were compared using a label-free analysis method. Mascot v.2.5 (Matrix Science, Boston, MA) was used for peptide identification searching against the sequence of the wild-type parent ATCC 17978 as reference [accession no. **GCA_000015425.1**, NCBI_Abaum_17978 17978_20160408 (3803 sequences; 1,121,966 residues)]. Scaffold v.4 (Proteome Software, Portland, OR) was used for protein filtering [protein false discovery rate (FDR) set to 1.0% and peptide FDR set to 0.1% with a two peptide minimum] and Progenesis LC-MS software (Nonlinear Dynamics, Durham, NC) was used for peak picking, peak alignment and quantification. Final data analysis was carried out using ratios of AB042 against ATCC 17978 using Microsoft Excel software (Microsoft Corp., Redmond, WA).

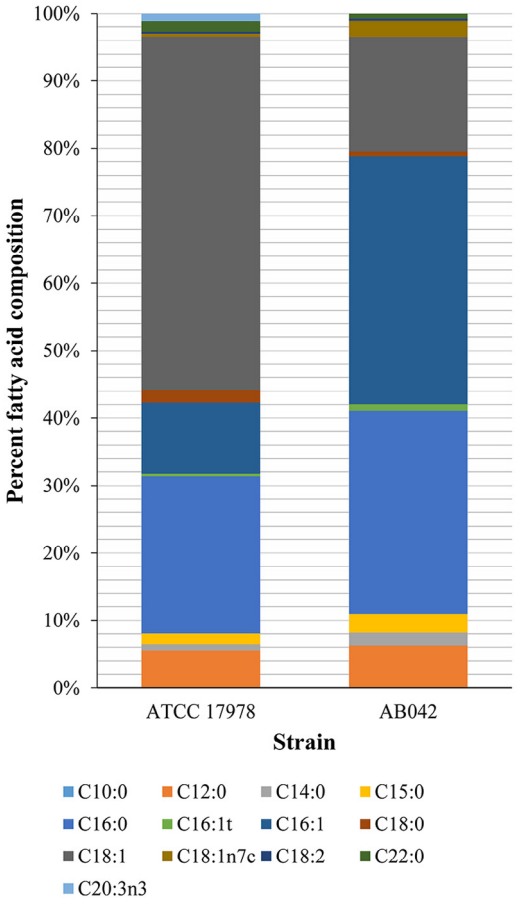

Fig. 1. Composition of fatty acids in *Acinetobacter baumannii* ATCC 17978 and the triclosan-resistant mutant strain AB042. Fatty acid composition was determined using cultures equilibrated to A_{600} = 1.0 using chromatography as described in Section 2.2. Data are representative of three biological replicates. A_{600}, absorbance at 600 nm.

3. Results

3.1. Fatty acid distribution is altered in A. baumannii AB042

A significant change in the fatty acid composition of AB042 was observed compared with the parent strain ATCC 17978 (Fig. 1). In particular, a decrease in C18:1 with a concomitant increase of C16:1 was observed in AB042, indicating a change in the membrane fatty acid composition in AB042 compared with ATCC 17978.

3.2. Genome sequencing reveals two single nucleotide mutations and a 73-bp deletion in the A. baumannii AB042 genome

Genome sequencing of AB042 using the PacBio platform and subsequent comparison with the parent ATCC 17978 confirmed a ^{31}D→N substitution (resulting from ^{91}g→a mutation) and a ^{96}G→V (resulting from ^{283}g→t mutation) substitution in FabB and FabI, respectively. In addition, there was a 73-bp deletion in *adeN*. These mutations have been described previously [15]. No additional mutations were observed in AB042.

3.3. Transcriptomics and proteomics analyses reveal upregulation in lipid transport, drug efflux and metabolism

Results of the transcription analysis are summarised in Fig. 2 and the complete results are included in Supplementary Table S1. The expression of 240 genes was altered ($P < 0.05$) (Supplementary Table S2), 68 of which were downregulated. COG (Clusters of Orthologous Groups) analysis of these 240 genes is shown in Fig. 3. A number of genes involved in lipid transport and metabolism (succinate-semialdehyde dehydrogenase, A1S_0853; ferredoxin-NADP reductase, A1S_0855; thioesterase, A1S_1367; putative acetyl-CoA acetyltransferase, A1S_1729; putative acetyl-CoA synthetase, A1S_2148; and putative fatty acid desaturase, A1S_2458) were overexpressed in AB042. Differential expression between AB042 and ATCC 17978 was also observed for genes involved in amino acid metabolism (A1S_1093 and A1S_1368-69-70). Expression of eight genes involved in carbohydrate metabolism was also altered, as was that of a number of membrane proteins, including RND protein (AdeJ, A1S_2736), ATP-binding cassette (ABC) transporter (A1S_1242), major facilitator superfamily (MFS) transporter (A1S_1257) and a glutamate transporter (A1S_1467). In addition, expression of genes believed to encode oxidoreductases (A1S_1368, A1S_1369 and A1S_1709) was also changed. Thirteen different transcriptional regulators were differentially expressed, with nine upregulated [A1S_0111 (LuxR family), A1S_0253 (TetR), A1S_0548 (TetR), A1S_1282 (CopG family), A1S_1371 (LysR family), A1S_1578 (AraC), A1S_2042 (TetR family), A1S_2219 (GntR family) and A1S_3264 (TetR family)] and four downregulated [A1S_0739 (TetR family), A1S_1539 (ArsR family), A1S_2456 (LysR family) and A1S_3262 (HxlR family)]. In addition, a number of genes that encode components of the type IV pili (A1S_2812, A1S_2813, A1S_3168, A1S_3193 and A1S_3194) were overexpressed. Furthermore, A1S_2811 was also overexpressed. This gene, located immediately upstream of type IV pili-encoding A1S_2812-3, encodes a histidine kinase and may potentially regulate their expression.

Analysis of the proteins using label-free analysis in AB042 identified 1305 proteins. A list of proteins whose expression is significantly altered in AB042 is provided in Table 1, whilst all of the proteins identified by this approach are listed in Supplementary Table S3. Expression of sulphate permease (A1S_3225) was the most highly overexpressed protein in AB042 relative to the wild-type ATCC 17978 (10.1-fold). Not surprisingly, AdeIJK proteins were also overexpressed (AdeI, 2.47-fold; AdeJ, 2.91-fold; and AdeK, 1.91-fold), confirming our data from RNA-Seq experiments as well as from the quantitative reverse transcriptase PCR that were as published previously [15]. Other proteins that were overexpressed included those involved in coenzyme transport and metabolism (A1S_0806, 2.57-fold and A1S_0807, 3.02-fold), lipid transport and metabolism (A1S_1421, 2.8-fold; A1S_2148, 2.33-fold; and A1S_2869, 1.81-fold) and those with unknown function (A1S_2203, 2.44-fold). The most downregulated targets belonged to amino acid transport and metabolism (A1S_1270, 2.99-fold) and translation (RNase P, A1S_2983, 2.57-fold).

4. Discussion

In this study, we describe the global impact of triclosan resistance in *A. baumannii*. We have previously shown that triclosan can select for mutants of *A. baumannii* that display reduced susceptibility to antibiotics [15]. Triclosan resistance has also been described in clinical isolates of *A. baumannii* [22], however whether triclosan resistance impacts treatment options for *A. baumannii* infections is not known. To get a better sense of global changes in protein expression in the mutant strain AB042, a multi-omics analysis was performed. The membrane composition of AB042 displayed a marked difference from the parent strain ATCC 17978, with a higher proportion of C_{16} fatty acids and a concomitant decrease in C_{18} fatty acids, something that has been described previously for diazaborine, an inhibitor of fatty acid biosynthesis [23]. We had sequenced AB042 in a previous study using the Illumina MiSeq platform. However, since we ended up with >300 contigs by this method, we decided to re-sequence AB042 using the PacBio platform. Analysis of the sequence confirmed single base pair mutations in *fabI* and *fabB*, respectively, and a 73-bp deletion in *adeN* previously reported [15].

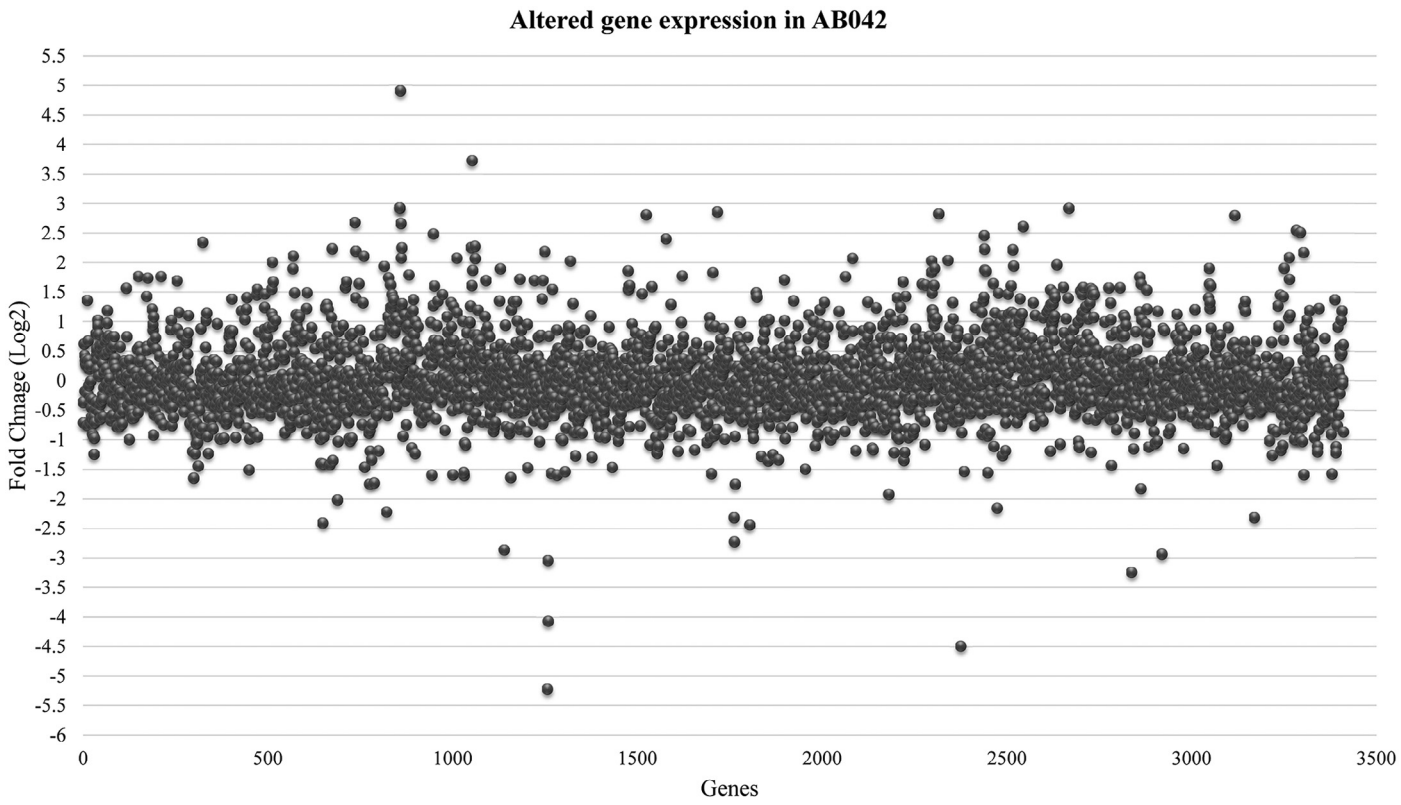

Fig. 2. Comparative transcriptomic analysis of *Acinetobacter baumannii* ATCC 17978 and the triclosan-resistant mutant strain AB042. Data show an overview of the differential gene expression (log_2 values) in AB042 compared with ATCC 17978 in cells at mid-log phase. Data shown are the mean of two biological replicates.

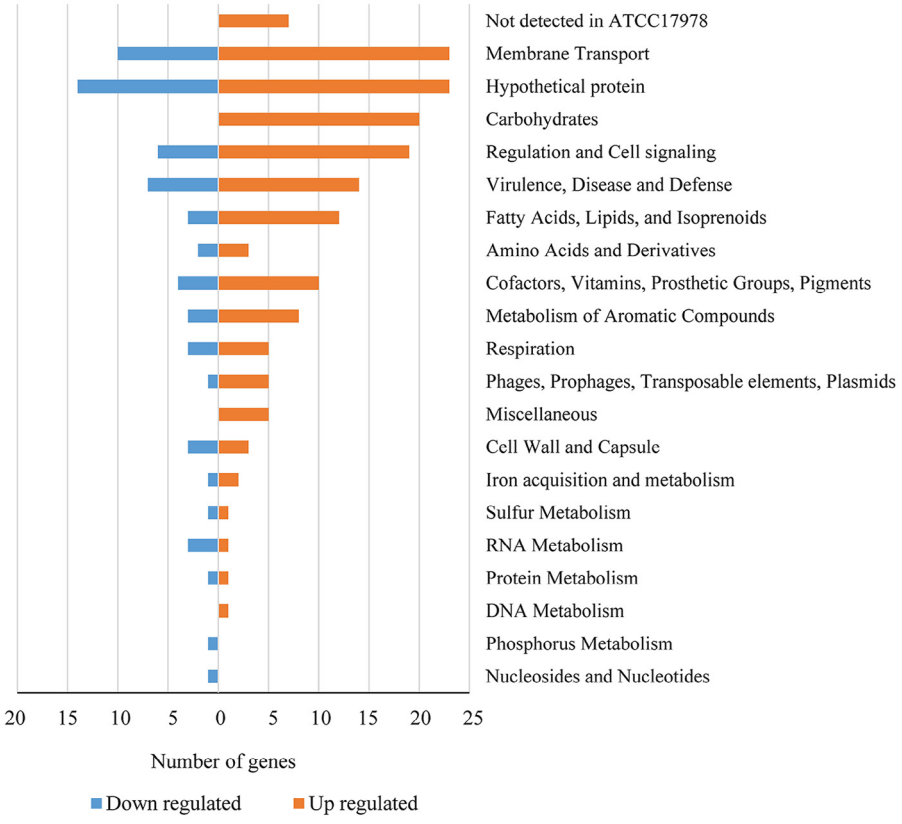

Fig. 3. COG (Clusters of Orthologous Groups) analysis of genes whose expression was significantly altered. Representation of genes whose expression was altered in *Acinetobacter baumannii* AB042 ($P < 0.05$) classified based on COG functions.

Table 1
Differential protein expression in *Acinetobacter baumannii* triclosan-resistant mutant AB042 compared with the wild-type ATCC 17978 parent strain, with $\log_2$ fold change cut-off greater than or equal to ±1.5 and $P < 0.05$.

Gene	Accession no.	Fold change ($\log_2$)[a]	Description
A1S_3225	CP000521.1_prot_ABO13616.2_3527	3.3	Putative sulphate permease
A1S_0807	CP000521.1_prot_ABO11245.2_841	1.6	8-Amino-7-oxononanoate synthase
A1S_2736	CP000521.1_prot_ABO13149.2_3006	1.5	AdeJ RND family drug transporter
A1S_1421	CP000521.1_prot_ABO11849.1_1540	1.5	Malonate decarboxylase α subunit
A1S_0806	CP000521.1_prot_ABO11244.2_840	1.4	Adenosylmethionine-8-amino-7-oxononanoate aminotransferase
A1S_2735	CP000521.1_prot_ABO13148.2_3005	1.3	AdeI
A1S_2203	CP000521.1_prot_ABO12630.2_2448	1.3	Hypothetical protein
A1S_2148	CP000521.1_prot_ABO12575.2_2388	1.2	Putative acetyl-CoA synthetase/AMP-(fatty) acid ligase
A1S_2737	CP000521.1_prot_ABO13150.2_3007	0.9	AdeK
A1S_0809	CP000521.1_prot_ABO11247.2_843	0.9	Dethiobiotin synthetase X
A1S_0534	CP000521.1_prot_ABO10987.2_513	0.8	NADH-dependent enoyl-ACP reductase
A1S_0975	CP000521.1_prot_ABO11407.1_1017	0.7	Hypothetical protein
A1S_3276	CP000521.1_prot_ABO13665.2_3582	0.6	Hypothetical protein
A1S_1966	CP000521.1_prot_ABO12393.2_2165	0.6	Hypothetical protein
A1S_3459	CP000521.1_prot_ABO13848.2_3786	0.6	Hypothetical protein
A1S_2145	CP000521.1_prot_ABO12572.2_2385	–0.6	Putative kinase
A1S_0445	CP000521.1_prot_ABO10900.1_424	–0.6	Hypothetical protein
A1S_3386	CP000521.1_prot_ABO13775.1_3704	–0.6	Phosphoserine phosphatase
A1S_0911	CP000521.1_prot_ABO11343.1_944	–0.6	Hypothetical protein
A1S_2041	CP000521.1_prot_ABO12468.2_2271	–0.6	Hypothetical protein
A1S_2956	CP000521.1_prot_ABO13359.2_3246	–0.7	Esterase
A1S_1281	CP000521.1_prot_ABO11709.2_1377	–0.7	TPR domain protein
A1S_3441	CP000521.1_prot_ABO13830.2_3765	–0.7	Putative signal peptide
A1S_0107	CP000521.1_prot_ABO10594.2_107	–0.7	Putative enoyl-CoA hydratase/isomerase family protein
A1S_0201	CP000521.1_prot_ABO10678.1_194	–0.8	Putative outer membrane protein
A1S_3417	CP000521.1_prot_ABO13806.2_3737	–0.8	Regulatory proteins IclR
A1S_0758	CP000521.1_prot_ABO11198.2_787	–0.9	NADH dehydrogenase I chain H
A1S_1267	CP000521.1_prot_ABO11695.2_1362	–1.1	Putative lactam utilisation protein
A1S_2262	CP000521.1_prot_ABO12685.2_2507	–1.2	EsvH
A1S_2983	CP000521.1_prot_ABO13386.2_3283	–1.5	RNase P
A1S_1270	CP000521.1_prot_ABO11698.2_1365	–1.6	Hypothetical protein
A1S_1269	CP000521.1_prot_ABO11697.2_1364	–1.8	Putative allophanate hydrolase subunits 1 and 2
A1S_1266	CP000521.1_prot_ABO11694.2_1361	–2.0	Putative membrane protein

[a] The mean of three biological replicates is shown.

The global impact of triclosan resistance in AB042 was analysed using transcriptomic and proteomic approaches. Whilst both these approaches are powerful tools to analyse the global changes in response to perturbations, they can have their limitations. For example, RNA-Seq, although a highly sensitive method, detects the abundance of transcripts that may not be a true representation of actual proteins in the cell. On the other hand, proteomics approaches lack sensitivity to detect low-abundance proteins [23]. Therefore, a combinatorial use of both of these approaches is likely to provide biologically relevant information especially since the correlation between the abundance of proteins with their corresponding mRNA is not strong and the variation can be as high as 60% [24].

We observed that the majority of genes with modulated expression were annotated as function unknown or hypothetical. As expected, some proteins involved in fatty acid metabolism were more highly expressed in AB042 relative to wild-type ATCC 17978. For example, expression of A1S_2148, which encodes the FadD (acyl-CoA synthase, fatty acid-CoA ligase) enzyme located in the inner membrane, was higher in AB042 than ATCC 17978. Its function is to activate fatty acids for decarboxylation through acylation of the fatty acid chain. This is the primary mechanism by which bacteria break down long chain fatty acids in the cell leading to breakdown into acetyl-CoA, which acts as a feeder pathway for fatty acid synthesis. In addition, RNA-Seq analysis also showed the upregulation of FadA subunit β (A1S_1731, 1.9-fold) and fatty acid desaturase (A1S_2458, 1.6-fold). FadA is required for dehydration and isomerisation of unsaturated fatty acids for feeding into fatty acid chain elongation [25]. Fatty acid desaturase (A1S_2458) catalyses the formation of double bonds in linoleoyl-CoA generating unsaturated fatty acids. What this may indicate is that apart from the previously characterised FabI mutation, changes in fatty acid metabolism overall may be modulated.

RNA-Seq data (Supplementary Tables S1 and S2) also showed the downregulation (2.2-fold) of the acyl-carrier protein phosphodiesterase (acyl-ACP) (A1S_1354). This protein is responsible for catalysing the removal of the 4′-phosphopantetheine group from CoA and has been shown to cleave acyl-ACP chains ranging from 6 to 16 carbons in length [26]. Its downregulation could result in the accumulation of C_{16} observed in fatty acid methyl ester (FAME) analysis. Changes to fatty acid composition in the membrane, including shortening of fatty acid length, were shown to modulate sensitivity to the antibiotic peptide warnericin RK in *Legionella pneumophila* [27]; whether a similar effect is observed in *A. baumannii* AB042 remains to be seen. Expression of A1S_1421 encoding malonate decarboxylase α subunit was upregulated (as detected both by transcriptomics and proteomics approaches). This protein is involved in the decarboxylation of malonate through exchange with acyl-carrier protein, resulting in the products of acetate and CO_2 [25,28].

Expression of A1S_3225, which encodes a putative sulphate permease, was upregulated as observed both through RNA-Seq and proteomics analysis. These MFS transporters, ubiquitous in eukaryotes and prokaryotes, function as proton:sulphate symporters [29]. These are involved in bringing inorganic sulphate anions into the cell and subsequently used in amino acid synthesis [30]. Notably, this protein has been shown to be a universal stress response protein in *A. baumannii* isolates [31,32] and therefore its overexpression in AB042 may also be a response to the stress caused by triclosan.

Biotin is the enzyme prosthetic group used by acetyl-CoA carboxylase to catalyse the two-step carboxylation of acetyl-CoA to malonyl-CoA. We observed the overexpression of three enzymes involved in biotin synthesis, the cofactor required for malonyl-CoA synthesis [33]. The three neighbouring genes A1S_0806 (adenosylmethionine-8-amino-7-oxononanoate aminotransferase), A1S_0807 (8-amino-7-oxononanoate synthase) and A1S_0809

(dethiobiotin synthase X) were overexpressed (Table 1). These enzymes are required for biotin synthesis, which is subsequently used as a co-factor for enzymes in fatty acid biosynthesis [34]. Dethiobiotin synthase X (A1S_0809) also catalyses a step in biotin synthesis; biotin is utilised as a cofactor by the acetyl-CoA carboxylase enzyme (AccD) [33]. Interestingly, the gene A1S_1270 that encodes a putative AccD-like protein was downregulated in this proteomics analysis and may be a propionyl-CoA carboxylase whose function in *Streptomyces coelicolor* is to produce methylmalonyl-CoA [35]. This metabolite does not get incorporated into fatty acids, but does require biotin for polyketide biosynthesis [35].

Furthermore, we also observed altered expression of at least 13 different transcriptional regulators (Supplementary Table S2). Examination of the genes encoded in the close vicinity of some of these regulators suggests that they may be involved in the regulation of membrane transporters and metabolism (fatty acid and amino acids). For example, A1S_1282 is located upstream of an ABC-type nitrate/sulphonate/bicarbonate transport system (A1S_1284); A1S_1539 is located upstream of a putative serine/threonine transporter (A1S_1538); A1S_2219 is located upstream of sodium/glutamate symport carrier proteins (A1S_2220-1); and A1S_2456 is upstream of genes encoding glycine, serine and threonine metabolism proteins (A1S_2454-3). Interestingly, A1S_2456 is also in the close vicinity of a fatty acid desaturase gene (A1S_2458). A1S_3262 is in the close vicinity of a putative acyl-transferase gene (A1S_3893). Furthermore, A1S_1371, a putative LysR-encoding gene (upregulated 1.23-fold), is located upstream of putative oxidoreductase-encoding genes (A1S_1369-70), whose expression was also found to be upregulated, indicating that A1S_1371 may be an activator of these two genes.

Previous studies on *Pseudomonas aeruginosa* show that triclosan treatment influences the expression of a number of genes involved in iron homeostasis [36] by creating a condition of excess intracellular iron leading to the downregulation of iron acquisition genes. Apart from a few genes [e.g. A1S_1655, a siderophore receptor protein (upregulated 1.3-fold), A1S_1361, an iron acquisition protein (upregulated 1.74-fold), and A1S_2042, a TetR-family transcriptional regulator (upregulated 1.19-fold) that is present upstream of a putative iron-regulated membrane protein (A1S_2043)], we did not observe altered expression of genes involved in iron metabolism in *A. baumannii*. Whilst it is possible that *A. baumannii* responds to triclosan in a different manner than *P. aeruginosa*, the difference may also stem from the fact that our experimental designs were not similar. The *P. aeruginosa* study involved exposing cells to triclosan for a short time and harvesting cells for analysis whilst triclosan was still present in the medium, whereas the current study was on cells that were mutated in the presence of triclosan but were not exposed to triclosan during any of the analysis. Therefore, the present study analyses the long-term effects of triclosan in *A. baumannii* ATCC 17978, whereas the *P. aeruginosa* study looked at the acute response to triclosan.

In this work, we show the global impact of triclosan resistance in *A. baumannii*. Using transcriptomics and proteomics analysis, we show that *A. baumannii* responds to triclosan by upregulating transporters, modulating fatty acid metabolism and overexpressing enzymes such as oxidoreductases.

Acknowledgments

The authors would like to thank Stuart McCorrister (Mass Spectrometry and Proteomics Core Facility, National Microbiology Laboratory, Winnipeg, MB, Canada) for mass spectrometry analysis and processing of the proteomics data.

Funding: This work was supported by the Discovery Grants program of the Natural Science and Engineering Council of Canada (NSERC) [RGPIN-2015-05550] and the University of Manitoba (AK). PL is funded by grants from the Canada Research Chair (CRC) program and NSERC [D9600]. MS is supported by the University of Manitoba Graduate Fellowship. The proteomics analysis was supported in part by the Public Health Agency of Canada.

Competing interests: None declared.

Ethical approval: Not required.

Appendix A. Supplementary data

Supplementary data associated with this article can be found, in the online version, at doi:10.1016/j.ijantimicag.2016.10.014.

References

[1] Lin MF, Lan CY. Antimicrobial resistance in Acinetobacter baumannii: from bench to bedside. World J Clin Cases 2014;2:787–814.
[2] Roca I, Espinal P, Vila-Farres X, Vila J. The *Acinetobacter baumannii* oxymoron: commensal hospital dweller turned pan-drug-resistant menace. Front Microbiol 2012;3:148.
[3] Gayoso CM, Mateos J, Mendez JA, Fernandez-Puente P, Rumbo C, Tomas M, et al. Molecular mechanisms involved in the response to desiccation stress and persistence in *Acinetobacter baumannii*. J Proteome Res 2014;13:460–76.
[4] de Breij A, Dijkshoorn L, Lagendijk E, van der Meer J, Koster A, Bloemberg G, et al. Do biofilm formation and interactions with human cells explain the clinical success of *Acinetobacter baumannii*? PLoS ONE 2010;5:e10732.
[5] Heath RJ, Rubin JR, Holland DR, Zhang E, Snow ME, Rock CO. Mechanism of triclosan inhibition of bacterial fatty acid synthesis. J Biol Chem 1999;274:11110–14.
[6] Heath RJ, Rock CO. Enoyl-acyl carrier protein reductase (*fabI*) plays a determinant role in completing cycles of fatty acid elongation in *Escherichia coli*. J Biol Chem 1995;270:26538–42.
[7] Heath RJ, Li J, Roland GE, Rock CO. Inhibition of the *Staphylococcus aureus* NADPH-dependent enoyl-acyl carrier protein reductase by triclosan and hexachlorophene. J Biol Chem 2000;275:4654–9.
[8] Webber MA, Randall LP, Cooles S, Woodward MJ, Piddock LJV. Triclosan resistance in *Salmonella enterica* serovar Typhimurium. J Antimicrob Chemother 2008;62:83–91.
[9] Chuanchuen R, Beinlich K, Hoang TT, Becher A, Karkhoff-Schweizer RR, Schweizer HP. Cross-resistance between triclosan and antibiotics in *Pseudomonas aeruginosa* is mediated by multidrug efflux pumps: exposure of a susceptible mutant strain to triclosan selects *nfxB* mutants overexpressing MexCD–OprJ. Antimicrob Agents Chemother 2001;45:428–32.
[10] Chuanchuen R, Narasaki CT, Schweizer HP. The MexJK efflux pump of *Pseudomonas aeruginosa* requires OprM for antibiotic efflux but not for efflux of triclosan. J Bacteriol 2002;184:5036–44.
[11] McMurry LM, Oethinger M, Levy SB. Overexpression of *marA*, *soxS*, or *acrAB* produces resistance to triclosan in laboratory and clinical strains of *Escherichia coli*. FEMS Microbiol Lett 1998;166:305–9.
[12] Curiao T, Marchi E, Viti C, Oggioni MR, Baquero F, Martinez JL, et al. Polymorphic variation in susceptibility and metabolism of triclosan-resistant mutants of *Escherichia coli* and *Klebsiella pneumoniae* clinical strains obtained after exposure to biocides and antibiotics. Antimicrob Agents Chemother 2015;59:3413–23.
[13] Lavilla Lerma L, Benomar N, Casado Munoz Mdel C, Galvez A, Abriouel H. Correlation between antibiotic and biocide resistance in mesophilic and psychrotrophic *Pseudomonas* spp. isolated from slaughterhouse surfaces throughout meat chain production. Food Microbiol 2015;51:33–44.
[14] Schweizer HP. Triclosan: a widely used biocide and its link to antibiotics. FEMS Microbiol Lett 2001;202:1–7.
[15] Fernando DM, Xu W, Loewen PC, Zhanel GG, Kumar A. Triclosan can select for an AdeIJK-overexpressing mutant of *Acinetobacter baumannii* ATCC 17978 that displays reduced susceptibility to multiple antibiotics. Antimicrob Agents Chemother 2014;58:6424–31.
[16] Sestric R, Munch G, Cicek N, Sparling R, Levin DB. Growth and neutral lipid synthesis by *Yarrowia lipolytica* on various carbon substrates under nutrient-sufficient and nutrient-limited conditions. Bioresour Technol 2014;164:41–6.
[17] Wattam AR, Abraham D, Dalay O, Disz TL, Driscoll T, Gabbard JL, et al. PATRIC, the bacterial bioinformatics database and analysis resource. Nucleic Acids Res 2014;42(Database issue):D581–91.
[18] Galardini M, Biondi EG, Bazzicalupo M, Mengoni A. CONTIGuator: a bacterial genomes finishing tool for structural insights on draft genomes. Source Code Biol Med 2011;6:11.
[19] Li H, Durbin R. Fast and accurate short read alignment with Burrows–Wheeler transform. Bioinformatics 2009;25:1754–60.
[20] Kim D, Pertea G, Trapnell C, Pimentel H, Kelley R, Salzberg SL. TopHat2: accurate alignment of transcriptomes in the presence of insertions, deletions and gene fusions. Genome Biol 2013;14:1–13.
[21] Trapnell C, Williams BA, Pertea G, Mortazavi A, Kwan G, van Baren MJ, et al. Transcript assembly and quantification by RNA-Seq reveals unannotated transcripts and isoform switching during cell differentiation. Nat Biotech 2010;28:511–15.

[22] Chen Y, Pi B, Zhou H, Yu Y-S, Li L. Triclosan resistance in clinical isolates of *Acinetobacter baumannii*. J Med Microbiol 2009;58:1086–91.
[23] Vogel C, Marcotte EM. Insights into the regulation of protein abundance from proteomic and transcriptomic analyses. Nat Rev Genet 2012;13:227–32.
[24] Maier T, Güell M, Serrano L. Correlation of mRNA and protein in complex biological samples. FEBS Lett 2009;583:3966–73.
[25] Fujita Y, Matsuoka H, Hirooka K. Regulation of fatty acid metabolism in bacteria. Mol Microbiol 2007;66:829–39.
[26] Thomas J, Cronan JE. The enigmatic acyl carrier protein phosphodiesterase of *Escherichia coli*: genetic and enzymological characterization. J Biol Chem 2005;280:34675–83.
[27] Verdon J, Berjeaud JM, Lacombe C, Hechard Y. Characterization of anti-*Legionella* activity of warnericin RK and delta-lysin I from *Staphylococcus warneri*. Peptides 2008;29:978–84.
[28] Chohnan S, Akagi K, Takamura Y. Functions of malonate decarboxylase subunits from *Pseudomonas putida*. Biosci Biotechnol Biochem 2003;67:214–17.
[29] Pao SS, Paulsen IT, Saier MH Jr. Major facilitator superfamily. Microbiol Mol Biol Rev 1998;62:1–34.
[30] Kertesz MA. Riding the sulfur cycle—metabolism of sulfonates and sulfate esters in Gram-negative bacteria. FEMS Microbiol Rev 2000;24:135–75.
[31] Šeputienė V, Povilonis J, Sužiedėlienė E. Novel variants of AbaR resistance islands with a common backbone in *Acinetobacter baumannii* isolates of European Clone II. Antimicrob Agents Chemother 2012;56:1969–73.
[32] Bonnin RA, Poirel L, Nordmann P. AbaR-type transposon structures in *Acinetobacter baumannii*. J Antimicrob Chemother 2012;67:234–6.
[33] Cronan JE Jr, Waldrop GL. Multi-subunit acetyl-CoA carboxylases. Prog Lipid Res 2002;41:407–35.
[34] Guchhait RB, Polakis SE, Dimroth P, Stoll E, Moss J, Lane MD. Acetyl coenzyme A carboxylase system of *Escherichia coli*. Purification and properties of the biotin carboxylase, carboxyltransferase, and carboxyl carrier protein components. J Biol Chem 1974;249:6633–45.
[35] Rodriguez E, Banchio C, Diacovich L, Bibb MJ, Gramajo H. Role of an essential acyl coenzyme A carboxylase in the primary and secondary metabolism of *Streptomyces coelicolor* A3(2). Appl Environ Microbiol 2001;67:4166–76.
[36] Chuanchuen R, Schweizer HP. Global transcriptional responses to triclosan exposure in *Pseudomonas aeruginosa*. Int J Antimicrob Agents 2012;40:114–22.